METALURGI
Majalah Ilmu dan Teknologi

EFFECT OF NICKEL ADDITION AND QUENCH-TEMPER PROCESS ON MECHANICAL AND CORROSION PROPERTIES OF ASTM A588 WEATHERING STEEL

Miftakhur Rohmah[a,*], Gilang Ramadhan[b], Dedi Irawan[a], Dedi Pria Utama[a], Toni Bambang Romijarso[a]

[a] Research Center for Metallurgy, National Research and Innovation Agency
Management Building 720, B.J. Habibie Sains and Technology Area, Banten, Indonesia 15314
[b] Departments of Metallurgical and Materials Engineering, Institut Teknologi Kalimantan
Jl. Soekarno Hatta KM 15, Balikpapan, Kalimantan, Indonesia
*E-mail: miftakhur.rohmah@brin.go.id

Abstract

Mechanical improvement and "self-protection" properties are mainly needed to develop weather-resistant steel materials. In this study, A588 steel was given thermomechanical treatment (hot-rolling) followed by a quenching-tempering process. The A588 steel is modified by adding 1, 2, and 3 wt.% nickel to the primary alloy. Steel is made using a hot rolling process at 1050 ℃ for 1 hour with 70% thickness reduction. The sample is heat-treated at 850 ℃ temperature for 1 hour and quenched in water, oil, and open air. The tempering process is conducted at 400 ℃ for 30 minutes. The metallography test confirmed the final microstructural and compared it with CCT (continuous cooling transformation) by Jmatpro simulation result. The fast cooling (water and oil quenchant) followed by the tempering process produces tempered martensite, ferrite, and pearlite, while the air-cooled forms a ferrite-pearlite. The cooling rate significantly affects strength and hardness and the nickel addition on hardness, and both factors have no significant on ductility. The sample owns the highest tensile strength value (~1226 MPa) with 1 %Ni, and the highest ductility value (around 17.1–27.43%) is obtained by air cooling. With 3% Ni, the corrosion rate decreases to 0.072 MPY with -432.5 mV for corrosion potential and 0.12μA/cm^{-2} for current density.

Keywords: A588, tempered martensite, cooling medium, nickel addition, quench-temper

1. INTRODUCTION

Nowadays, WS (weathering steel) is progressively popular in demand. Good weldability, high strength, and good resistance to atmospheric corrosion due to the patina layer formed are the reasons for many enthusiasts of weather-resistant steel materials. WS is designed as low-alloy steel because the carbon level is kept under 0.2%, and the total amount of alloying elements of Cu, P, Cr, Ni, Mn, and Si did not exceed 5% [1]. As a used connection for bridge steel structures, high-strength bolts are predominantly made of medium carbon alloy steel, and weathering steel is rarely used. Therefore, it is urgent to develop special high-strength bolts for the atmospheric environment. The national steel industry is expected to produce

WS using local raw materials, independently. Alternative sources of high-grade iron ore, such as laterite ore processed into laterite steel, are critical to meeting Indonesia's demand for weathering steel.

The nickel content of traditional WS is generally less than 0.4%. The last study affirmed that the Ni addition of up to 1% in the conventional WS will reduce the hot shortness during the rolling process and improve the corrosion resistance [2]. Cheng et. al., [3] claimed that nickel not exceeding 3.5% induces fine crystalline formation-compact rust and increases the ratio of α/γ FeOOH in acidic and marine atmospheric. Therefore, the weathering steel design not only focuses on its weathering characteristics but should also comprehensively

consider the strength, elasticity, and ease of processing.

To achieve the desired combination of strength and elasticity, WS must be quenched and tempered with minimal residual stress, distortion, and crack formation. Quenching effectiveness is dependent on the steel composition, type of quenchant, or the quenchant use condition [4]. Also, the tempering temperature is one of the critical roles of microstructural evolution, carbide formation, and coarsening behavior, which influences the mechanical properties [5]-[6]. Tempering temperature, holding time, and cooling rate from the tempering temperature significantly affect steel's final properties. As the previous study, the low temperature (150 °C) of the tempering process caused the fine carbide deposition and the phase transformation of martensite to bainite in small quantities, so it is no significant impact on strength and elongation [7]. Besides that, the influence of alloying elements on mechanical and corrosion behavior is convoluted. Chen et. al., [8] inferred that high tempering temperature causes the carbide forming element (Cr dan Mn) to be enriched in the cementite, while the non-carbide forming element (Ni) is rejected from the cementite.

Although the mechanical properties of WS can be estimated from the composition, the effect of quench-temper has few reported previously. Atapek et. al., [9] showed that the steel-tempered microstructure directly affects corrosion. When these steel are immersed in NaCl solution, the anodic dissolution starts along the amorphous grain boundary within the martensitic matrix. Martensite has a deleterious effect on electrochemical corrosion due to residual stress and the formation of micro-galvanic corrosion between martensite and the other phase [10].

In this study, the quench-temper experiment was carried out on the A-588 modified. Media quenchant variation was investigated, corresponding to the relationship between microstructure, mechanical, and corrosion properties. The primary purpose of this experiment is to provide proper media quenching at specific compositions and the development of high-strength steel to broaden its industrial application.

2. MATERIALS AND METHODS

Lateritic steel was created through the refining and re-melting of NPI (nickel pig iron). Scraps and alloying elements (ferromanganese, ferrosilicon, nickel, copper, vanadium, and tungsten) were melted in an induction furnace at 1700 - 1800 °C. The primary composition was based on the ASTM A-588 standard. The alloying effect was determined by modifying the molten metal by adding 1, 2, and 3 wt.% Ni to the primary alloy composition. Table 1 shows the chemical composition obtained from an OES (optical emission spectroscopy) test.

Table 1. Chemical composition of ASTM A588 (wt.%)

Elements	Samples Code			
	A	**B**	**C**	**D**
C	0.177	0.177	0.161	0.161
Al	0.02	0.05	0.19	0.016
S	0.0026	0.0024	0.0030	0.0024
Cr	0.49	0.49	0.50	0.51
Mn	1.08	1.06	1.01	1.07
Ni	0.41	1.21	1.95	2.91
P	0.011	0.001	0.014	0.001
Cu	0.32	0.34	0.32	0.32
Si	0.43	0.41	0.32	0.37
V	0.064	0.064	0.062	0.062
Fe	Bal.	Bal.	Bal.	Bal.

Casted ingot steel was homogenized at 900 °C for a few hours to remove a dendritic structure. The ingot was cut into 10 x 5 x 1 cm^3 of dimension, which is then used as rolling samples. The hot rolling process was performed by heating at 1050 °C for 1 hour. The hot rolling was carried out in 2 cycles to obtain a thickness reduction of 70% and a final plate thickness of 0.3 cm. Then, the samples were given a heat-treatment process by austenitized at 850 °C for 1 hour and subsequently quenched into different media to obtain martensite structure. The quenching media used are water, oil, and open air. Jmat-Pro software predicted the martensitic start temperature. In addition, the martensite and bainite start were estimated by Eq.1-2 [11]-[12]. The tempering process was conducted at 400 °C for 30 minutes. The sequence of heat treatment processes was schematically shown in Fig. 1.
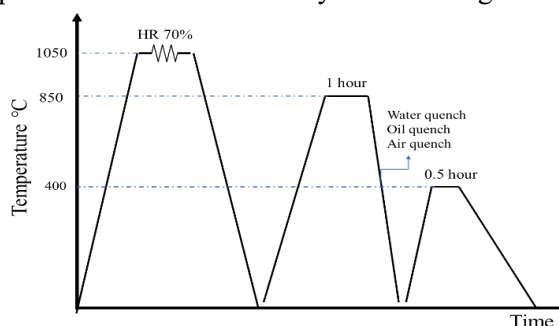
Figure 1. Schematic diagram of heat treatment process on modified laterite steel A-588

A metallographic test was used for confirmed the microstructure. Before the test, the samples were prepared by cut into 5 x 5 mm, mounted with epoxy resin, wet-ground with SiC papers (80-1200 grit gradually), and polished with alumina slurry (5 and 1 μm). After

obtaining a like mirror surface without a scratch, they were etched with a picral solution to reveal microstructure. The volume fraction of the phase was determined using the systematic manual Point Count method, prescribed in the ASTM standard E562.

$$Ms\,(^{o}C) = 539 - 423C - 30.4Mn - 12.1 - 17.7Ni - 7.5Mo\,(wt.\%) \qquad (1)$$

$$Bs\,(^{o}C) = 656 - 57.7\,C - 35Mn - 75Si - 15.3Ni - 34\,Cr - 41.2Mo\,(wt.\%) \qquad (2)$$

The tensile and hardness test was used to determine mechanical properties. The hardness measurement was carried out by the Brinell method with 1000 kgf of indentation for 10 seconds. The samples were prepared according to the ASTM E8 standard for the tensile test.

A polarization test confirmed the corrosion properties in NaCl 3.5% solution at room temperature. The test was conducted at the cell-system electrode. The three electrodes consist of SCE (saturated calomel) as a reference, the Platine wire as counter, and the sample as a working electrode. The swept potential was used from -200 to +200 mV with 1mV/s of scan rate.

3. RESULT AND DISCUSSION
3.1 CCT Diagram of Laterite Nickel-Based A588 Alloy Steel

The CCT (continuous cooling transformation) diagram shows the possibility of each alloy forming a different phase: austenite, ferrite, pearlite, bainite, and martensite. The phase distribution in all samples depends on the cooling rate, temperature, and holding time. CCT diagram images from the simulation of the JMatPro software are shown in Fig. 2.

From the CCT diagram in Fig. 2, the Ni addition significantly affects the ferrite phase (black line) formed and has little impact on other phases such as pearlite (light green line), bainite (blue line), retained austenite (dark green line) and martensite (thin purple line). The ferrite and retained austenite phases were formed with a cooling rate of 1 to 5 in sample A (Fig. 2(a)) and underwent a significant shift in sample D (Figure 2d). In Sample A, the starting line for the ferrite and austenite formation lies in the same period (cooling rate region 1).
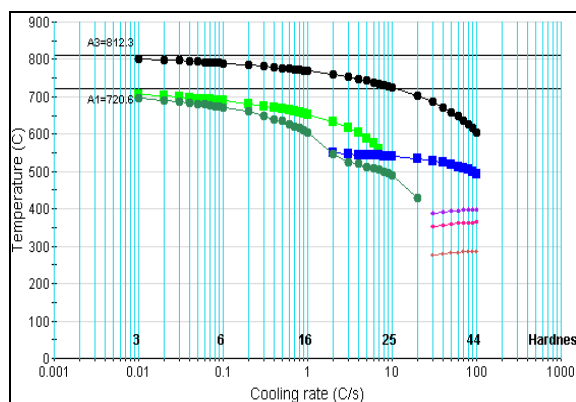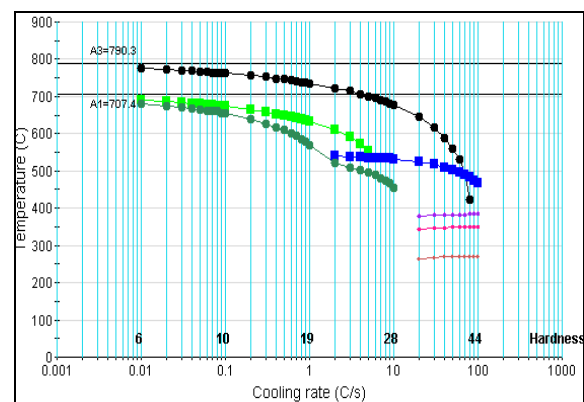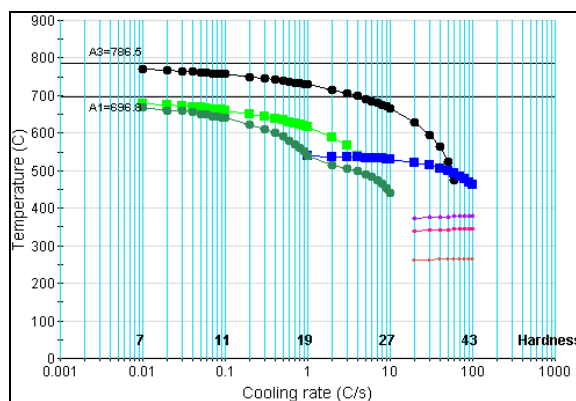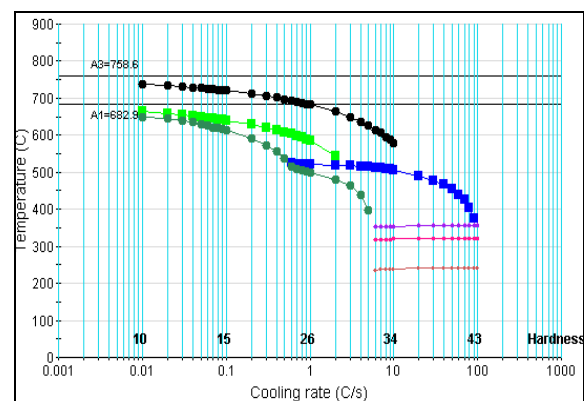
Figure 2. CCT (continuous cooling transformation) diagrams for: (a) Sample A (0.41 wt.% Ni); (b) Sample B (1 wt.% Ni); (c) Sample C (2 wt.% Ni); (d) Sample D (3 wt.% Ni)

As the Ni content increased from Sample B to Sample D, ferrite and austenite formation moved at different timescales and tended longer. The addition of 3 wt.% Ni shifted the ferrite and austenite areas towards the slower cooling rate line and increased the bainite area. As a result, ferrite and retained austenite will only form heat treatment in the cooling rate region 2 of sample D. This shift in the ferrite area towards the slower cooling rate line indicates that increasing the Ni content expands the austenite area.

Nickel is a stabilizer of austenite and can reduce the critical cooling rate of bainite formation [13]. Mo, Cr, and Ni are responsible for broadening the bainitic transformation region and obtaining bainitic fraction after quenching [14]. The presence of nickel shifts the CCT curve to the right, thus delaying the reaction of ferrite, pearlite, and bainite [7]. In this simulation, the addition of Ni will affect the formation of bainite with a range of cooling rates towards a slower cooling rate, which is around 0.6 °C/s to 100 °C/s. For the martensite formation, the addition of Ni in each sample resulted in a change in area by shifting the initial line of transformation to a lower temperature. Ms (Martensite Start) was calculated to be 398 °C for sample A and decreased to 355 °C for sample D. This indiciated that the low-temperature bainite was successfully attained by increasing the nickel [15]. Based on the CCT results, the initial temperatures of martensite and bainite are shown in Table 2.

Table 2. The calculated of martensite and bainite start temperature in A588 steel from JMatPro software simulation

Sample Code	Ni content (wt.%)	Martensite Start (°C)	Bainite Start (°C)
A	0.41	398	553
B	1.21	383	539
C	1.95	378	540
D	2.91	355	523

3.2 Microstructure Analysis

The microstructure of A588 steel based on nickel laterite with variations in cooling is shown in Fig. 3. Figure 3 shows the effect of media quenchant (water, oil, and open-air cooling) on the A588 microstructure after the quench-temper process. In general, the microstructure of the water-oil quenched subsequently a tempered process was consisting of tempered martensite or bainite (finer needle lathe-like structure), fine pearlite (black color lamellar structure), and ferrite (white light color). The microstructure of water quench (Fig. 3(a)) consists of 24% ferrite, 57% tempered martensite, and 19% pearlite, whereas the oil quench (Fig. 3(b)) consists of 62% tempered martensite, 22% ferrite, and 16%

pearlite. This difference in phase fraction results in higher strength values and lower ductility than air cooling.

(a)

(b)

(c)
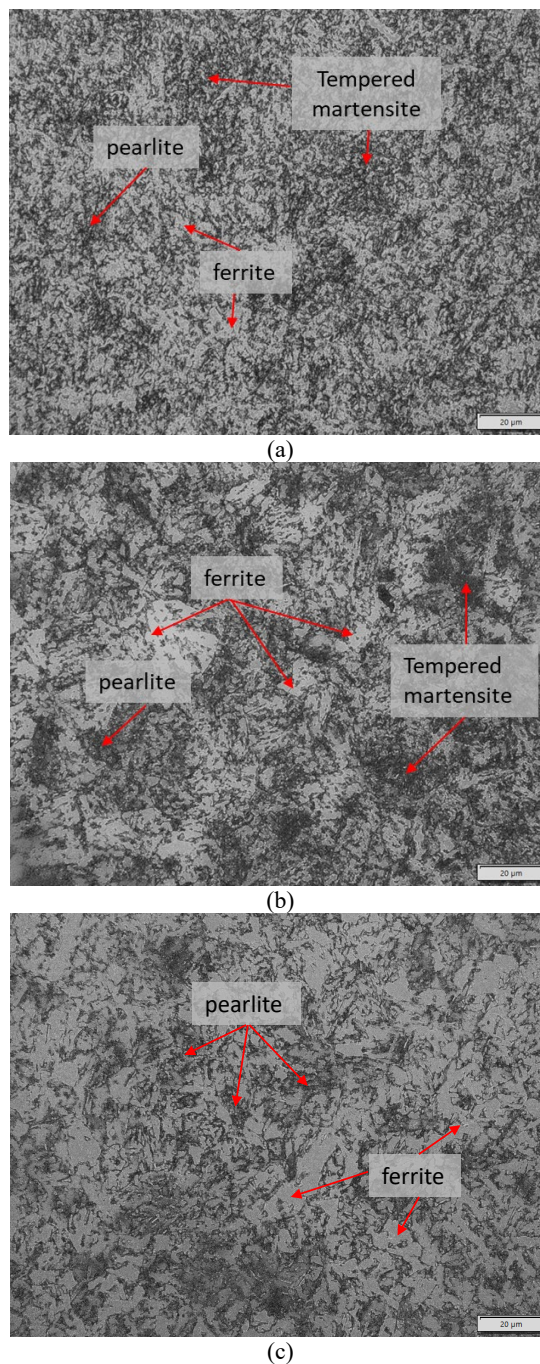
Figure 3. Microstructure of A588 steel with a composition of 0.42% Ni after quench-temper process with cooling media of (a) water, (b) oil, and (c) open air. Etching with Picral solution

The tempered martensite, which consists of recrystallization ferrite (equiaxed α phase) and cementite phase, is formed as a result of single-phase martensite (BCT-body centered tetragonal) saturated with carbon undergoing a reaction due to low energy activation for diffusion during reheating process [16]-[17]. As a result of the tempered martensite formation, the mechanical properties are not as hard as martensite but more

ductile than martensite [17]. As tempered at 400 ℃, the ferrite increases due to the reduction in the martensite phase and facilitates the fine pearlite precipitation. Quench media is closely related to cooling rate and residual stresses formed due to carbon supersaturated solute atoms during cooling [18]. The water and oil quenchant leads to rising in cooling rate more than air cooling and accelerates the austenite decomposition into martensite form (tetragonal structure) with diffusion-less transformation. But, slow cooling within the materials leads to the laminar phases of pearlite, bainite, and ferrite [19]. In lower C concentration (0.17 wt.%C), tempering 400 ℃ will improve the ductility and young modulus due to the different shear modulus of tempered martensite, which simultaneously leads to generating the prevalent unstable martensite structure, ferrite, cementite, and a carbide precipitate, which associated with the change in lattice distortion (BCT to BCC-body centered cubic lattice).

However, as the carbide particle expands during the dislocation process under tensile force, the shearing stress rises as well [20]. Oil-tempered martensite has a different form than water-cooled tempered martensite. It is because the cooling rate of oil is slightly slower than that of water. As a result, this affects the transformation time of austenite into martensite so that the resulting martensite becomes larger and tends to form blocks. Like the water quenched, austenite does not have enough time to transform into the ferrite phase. As a result, the final martensite is smaller than the martensite with oil cooling [7]. The tempered martensite was not visible (Fig. 3(c)) on decreasing the cooling rate of heat treatment i.e., with open-air cooling. The tempering process does not alter the microstructure of ferrite and pearlite.

Figure 4 shows the nickel content effect on the microstructure of A588 steel. In general, the microstructure consisted of tempered martensite (bainite form or needle-like structure in the black part), ferrite, and pearlite. As increasing the nickel, the grain size increased and the irregular block of bainite was observed (Figs. 4(c)-4(d)) [15]. With the increase of nickel level, the coarse austenite was more likely formed and provided a driving force for the bainite growth. Therefore, there is a large amount of bainite in the sample with 3% Ni [15],[21].
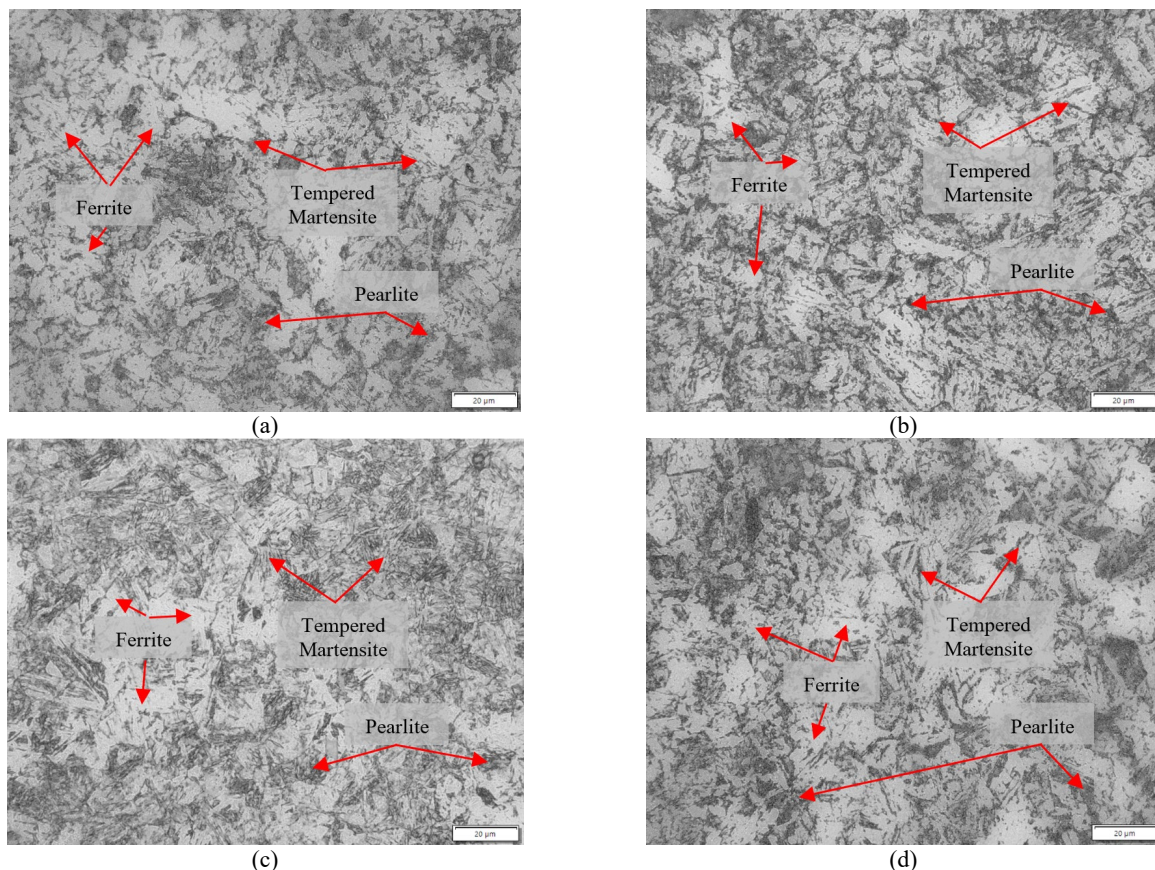
Figure 4. The effect of nickel level of (a) 0.41%, (b) 1%, (c) 2%, and 3% after water quench and followed by tempering at 400 ℃. Etching with Picral solution

The bainite structure is formed as a result of austenite transformation during water quench (according to Fig. 2) while martensite is transformed to tempered martensite (mixture of ferrite+cementite) during tempering at 400 ℃.

3.2 Mechanical Properties

The mechanical properties of A588 with nickel addition in varying quench was successfully represented by tensile and hardness test. The tensile result is shown in Fig. 5, and the hardness result is shown in Fig. 6.

(a)

(b)
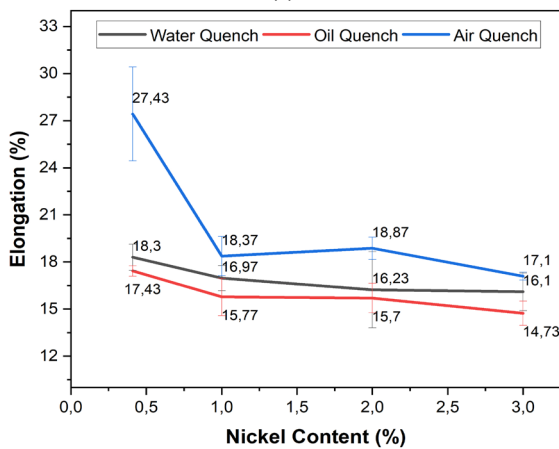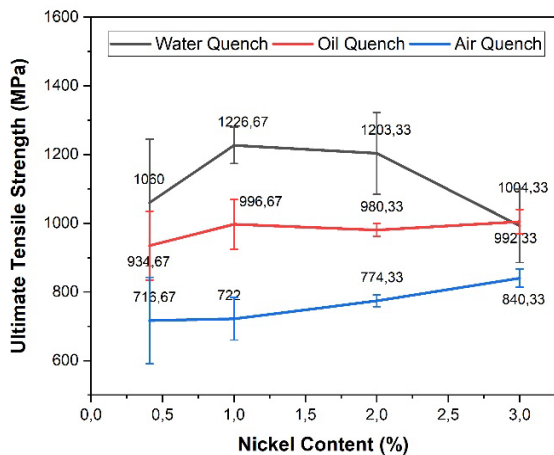
Figure 5. Effect of nickel and quenchant medium on (a) ultimate tensile strength and (b) elongation of A588 steel

Based on Figure 5, the cooling medium significantly affects the strength value in A588, while the nickel addition is slightly affected. The fast cooling, i.e. water quench, produces the highest strength value compared to other cooling media, is 1060 Mpa for 0.41% Ni, 1226.67 for 1% Ni, 1203.33 MPa for 2% Ni, and 1004.33 MPa for 3% Ni. The strength increases considerably with the cooling rate during quenching. By reducing the martensite transformation temperature and producing enormous martensite (high volume phase), nickel is a common austenite stabilizer which

subsequently increases strength in an indirect manner [22]. Also, UTS can be strengthened using a substitusional solid solution. This result follows the simulation using JMAtPro software that the faster the cooling rate, the less perfect the sample will diffuse and resulting in the presence of a martensite phase [16].
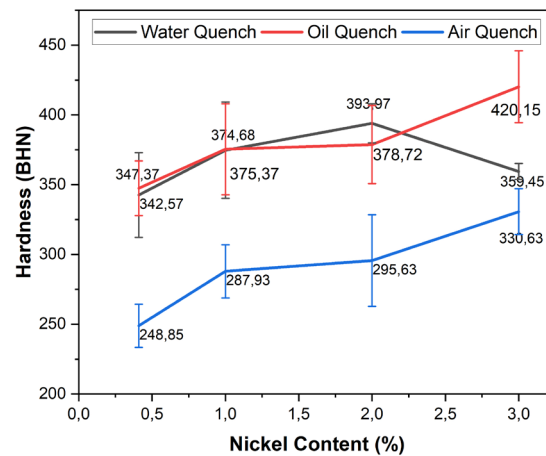
Figure 6. Effect nickel and quenchant medium on hardness of A588 steel

In opposition, the excessive nickel could also increase the stability of retained austenite, increase carbon's activity coefficient, and further decrease strength [23]. With fast cooling, the nickel addition improves the strength to 1226.67 MPa for water quenched and 996.67 MPa for oil quenched.

In addition, the rule of ductility is inversely proportional to the value of tensile strength. As increase the cooling rate, the elongation decreases. The air-quenched sample had the highest elongation the other, which is 17.1–27.43%. Air-quench allows the austenite phase to diffuse more entirely to have a more ductile phase and form a ferrite-pearlite phase. The tempered martensite did not carry excellent strength and microhardness, but its plasticity and toughness are relatively better [16].

In low alloy, the tempering process induces the decomposition of tempered martensite, static recovery of dislocation, and residual stress released. The ductility after quenching is close to the air cooling value. Besides that, the nickel addition causes a slight decrease in the ductility value due to the high fraction of martensite.

In Figure 6, the water and oil quenched samples had a similar hardness of above 340 BHN, and the air-quenched sample had a lower hardness of 240-330 BHN. The hardness results have a similar pattern to the strength value. During the 400 ℃ tempering process, the diffusion kinetics of atoms is feasible, which results in a moderate rate of softening effect [18].

The results obtained for tensile and hardness are subjected to statistical analysis using the ANOVA (analysis of variance) - two ways factor with a 5% significance level.

Table 3. Result of ANOVA-two way for strength

	DF	Sum of Squares	Mean Square	F Value	P Value
Nickel Addition	3	13160.84	4386.95	0.694	0.588
Cooling Medium	2	258914.02	129457.01	20.486	0.002
Error	6	37916.13	6319.35		
Total	11	309990.99			

The F-critical is 4.757 for nickel addition and 5.143 for the cooling medium factor. If the F-value < F-critical, the nickel addition or cooling medium aspect is not affected. On the contrary, if the F-value > F-critical, the nickel addition or cooling medium significantly affects the properties.

Table 4. Result of ANOVA-two way for elongation

	DF	Sum of Squares	Mean Square	F Value	P Value
Nickel Addition	3	45.74	15.25	3.278	0.101
Cooling Medium	2	45.44	22.72	4.884	0.055
Error	6	27.91	4.65		
Total	11	119.09			

The ANOVA results in Table 3-5 show that the nickel addition does not significantly affect the strength, but the cooling medium factor is worked substantially on. It is indicated that the microstructure differences after the quench-temper have to involve the strength value considerably, while the grain size does not. In addition, elongation is not significantly affected by cooling media and nickel addition.

Table 5. Result of ANOVA-two way for hardness

	DF	Sum of Squares	Mean Square	F Value	P Value
Nickel Addition	3	5325.98	1775.33	4.864	0.048
Cooling Medium	2	18815.03	9407.51	25.774	0.001
Error	6	2189.97	364.99		
Total	11	26330.98			

The ductility value of the oil-water quench sample is almost equivalent to that of air cooling. The hardness is greatly influenced by cooling and nickel level differences.

3.3 Corrosion Properties in 3.5% NaCl

The corrosion behavior of steel mainly depends on chemical composition and microstructure. The corrosion of tempered A588 steel in 3.5 wt% NaCl solution was examined
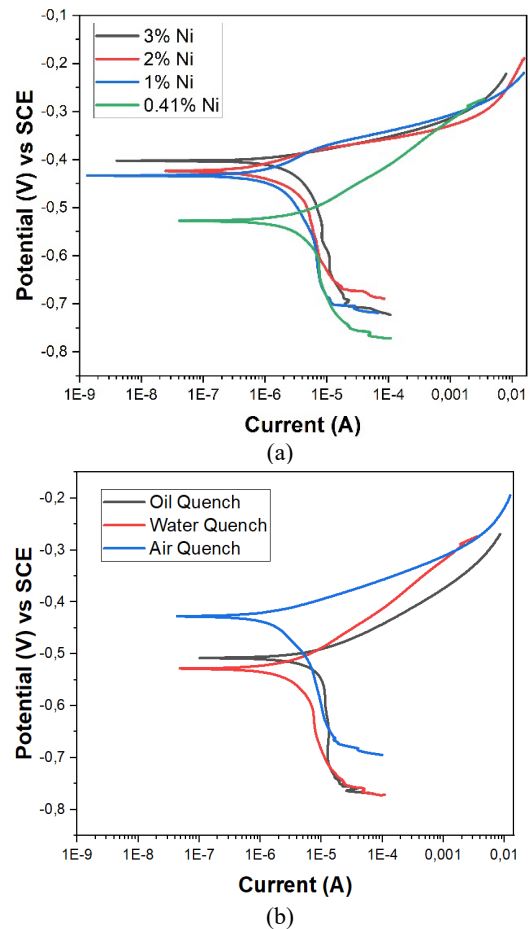
Figure 7. Effect of (a) nickel addition and (b) cooling media on the polarization curve of A588 steel

using the Tafel extrapolation technique, shown in Fig 7. The electrochemical parameter obtained from the extrapolation of anodic and cathodic Tafel fit lines are listed at Table 6.

From Figure 7(a), the nickel addition in tempered A588 steel shifted the curve upward and remarkably changed the corrosion potential ($Ecorr$) – current corrosion ($Icorr$).

Table 6. The fitted value of the polarization paramater of A588

	Beta (x10^{-3} V/dec)	Ecorr (mV)	Icorr (µA/cm^2)	Corrosion Rate (mpy)
0.41% Ni - Water quench	533.8	-528.0	5.343	2.879
1% Ni - water quench	618.7	-471.8	4.940	2.697
2% Ni - water quench	481.7	-424.6	3.336	1.944
3% Ni - water quench	26.26	-432,5	0.12	0.072
0.41% Ni - Oil quench	58.19	-508.9	7.728	4.504
0.41% Ni - Air Quench	38.13	-427.6	1.443	0.841

The corrosion current density (*Icorr*) decreased from 5.343 µA/cm^2 to 0.12 µA/cm^2 with the nickel addition of up to 3%. With the increase of nickel level, the mixed-corrosion potential tends to be more positive, and further, the corrosion rate became slower. The less positive potential probably indicates the higher ability of 3%Ni in developing a thicker layer of corrosion product compared to 0.41% Ni [24]. Besides that, the grain size of the bainite phase (Figs. 4(a)-4(d)) also works on the corrosion rate. The more refined martensite structure could improve corrosion resistance [25].

The cooling medium influences the polarization curve shifting according to Fig. 7(b). As the cooling rate increase, the curve moves downward and Icorr becomes more negative. It indicates that the corrosion rate increases from 0.841 to 4.504 mpy as the cooling rate accelerates. The pearlite was preferably corroded, and the lamellar Fe$_3$C inside the pearlite/bainite structure could push forward the Fe^{2+} dissolution because the pearlite's zero current potential is more negative than ferrite. After the pearlite phase was totally corroded, the corrosion entered the ferrite phase from the ferrite/pearlite phase boundary. It was noticed that the multiphase formed a micro-galvanic between martensite island with bainite-ferrite couple corrosion and advanced the higher corrosion [25]. Compared with bainite and martensite, pearlite has better corrosion resistance.

The difference in volume fraction of each phase in the oil and water quenched sample causes differences in the corrosion rate. Tempered martensite of volume fraction plays a vital role in the corrosion mechanism, and the martensite phase is less noble than the bainite phase. The corrosion is preferred to occur at the interface and the lath of tempered martensite with high grain boundary [26]-[27]. The oil-quenched sample has a higher martensite volume fraction (Fig. 3(a)-3(b)), so the corrosion is more aggressive than a water-quench sample.

4. CONCLUSION

The combined effects of nickel addition and the quench-temper method on the mechanical and corrosion properties of A-588 steel were examined in this study. Nickel is a typical austenite stabilizer that indirectly boosts strength by lowering the martensite transformation temperature and creating large martensite. Bainite's and martensite's temperature is often lowered when nickel is added up to 3%, to 355 for Ms and 523 for Bs, respectively. Due to the out-diffusion of carbon, the ferrite fraction increases as the temperature is tempered to 400 by rapid cooling (water and oil quenchant). Its favors the formation of fine cementite (tempered martensite). The air quench-temper method was used to create the ferrite-pearlite structure. The tensile strength value and the ductility rule have an inverse relationship. The water quench prepared the strongest specimens, and its strength increases with the addition of 1% nickel (1226.67 MPa), but it drops to 1004.33 MPa when an excess of 3% nickel is applied due to the increased retained austenite. The elongation (%) decreased as the cooling rate increased, typically 17.43-14.73 for oil quench, 18.3-16.1 for water quench, and 27.43-17.1 for open-air cooling. The addition of nickel had no impact on the strength and elongation, according to the results of the ANOVA statistical test; however, the change of the cooling medium significantly impacted the tensile properties (P values 0.588 and 0.101). The hardness of the water- and oil-quenched samples were both above 340 BHN, while the hardness of the air-quenched sample was between 240 and 330 BHN. Both factors have a significant impact on hardness.

REFERENCES

[1] J. Jia, Z. Liu, X. Cheng, C. Du, and X. Li, "Development and optimization of Ni-advanced weathering steel: A review," *Corros. Commun.*, vol. 2, pp. 82-90, 2021. Doi: 10.1016/j.corcom.2021.09.003.

[2] M. Morcillo, I. Díaz, H. Cano, B. Chico, and D. de la Fuente, "Atmospheric corrosion of weathering steels. Overview for engineers. Part I: Basic concepts," *Constr. Build. Mater.*, vol. 213, pp. 723-737, 2019. Doi: 10.1016/j.conbuildmat.2019.03.334.

[3] X. Cheng, Z. Jin, M. Liu, and X. Li, "Optimizing the nickel content in weathering steels to enhance their corrosion resistance in acidic atmospheres," *Corros. Sci.*, vol. 115, pp. 135-142, 2017. Doi: 10.1016/j.corsci.2016.11.016.

[4] S. . Tukur, M. M. Usman, I. Muhammad, and N. A. Sulaiman, "Effect of tempering temperature on mechanical properties of medium carbon steel," *Int. J. Eng. Trends Technol.*, vol. 9, no. 15, pp. 798-800,

2014. Doi: 10.14445/22315381/ijett-v9p350.

[5] Y. K. Bao, M. Wu, K. X. Liu, Y. Y. Feng, and X. M. Zhao, "Effect of tempering temperature on carbide precipitation and mechanical properties of marine atmospheric corrosion resistant steel," *J. Mater. Eng. Perform.*, vol. 31, pp. 2517-2524, 2022. Doi: 10.1007/s11665-021-06335-6.

[6] D. Ning, C.R. Dai, J. L Wu, Y.D Wang, Y.Q Wang, Y. Jing, and J. Sun., "Carbide precipitation and coarsening kinetics in low carbon and low alloy steel during quenching and subsequently tempering," *Mater. Charact.*, vol. 176, pp. 111111, 2021. Doi: 10.1016/j.matchar.2021.111111.

[7] M. Rohmah, D. Irawan, D. P. Utama, and T. B. Romijarso, "Pengembangan baja laterit modifikasi A588 menggunakan proses termomekanikal diikuti dengan proses temper temperatur rendah untuk aplikasi baja tahan cuaca," *TEKNIK*, vol. 42, no. 2, pp. 149-159, 2021. Doi: 10.14710/teknik.

[8] C. Zhu, X. Y. Xiong, A. Cerezo, R. Hardwicke, G. Krauss, and G. D. W. Smith, "Three-dimensional atom probe characterization of alloy element partitioning in cementite during tempering of alloy steel," *Ultramicroscopy*, vol. 107, no. 9, pp. 808-812, 2007. Doi: 10.1016/j.ultramic.2007.02.033.

[9] Ş. H. Atapek, Ş. Polat, and S. Zor, "Effect of tempering temperature and microstructure on the corrosion behavior of a tempered steel," *Prot. Met. Phys. Chem. Surfaces*, vol. 49, no. 2, pp. 240-246, 2013. Doi: 10.1134/S2070205113020111.

[10] A. Kalhor, M. Soleimani, H. Mirzadeh, and V. Uthaisangsuk, "A review of recent progress in mechanical and corrosion properties of dual phase steels," *Arch. Civ. Mech. Eng.*, vol. 20, no. 3, pp. 1-14, 2020. Doi: 10.1007/s43452-020-00088-0.

[11] Y. K. Lee, "Empirical formula of isothermal bainite start temperature of steels," *J. Mater. Sci. Lett.*, vol. 21, no. 16, pp. 1253-1255, 2002. Doi: 10.1023/A:1016555119230.

[12] J. Platl, H. Leitner, C. Turk, and R. Schnitzer, "Determination of martensite start temperature of high-speed steels based on thermodynamic calculations," *Steel Res. Int.*, vol. 91, no. 8, 2020. Doi: 10.1002/srin.202000063.

[13] H. Martin, P. A. Yirenkyi, A. Pohjonen, N. K. Frempong, J. Komi, and M. Somani, "Statistical modeling for prediction of CCT diagrams of steels involving interaction of alloying elements," *Metall. Mater. Trans. B Process Metall. Mater. Process. Sci.*, vol. 52, no. 1, pp. 223-235, 2021. Doi: 10.1007/s11663-020-01991-w.

[14] R. Neugebauer, A. Rautenstrauch, and E. Meza-García, "Influence of the alloying elements on phase transitions of high strength steels," *Adv. Mater. Res.*, vol. 337, pp. 358-362, 2011. Doi: 10.4028/www.scientific.net/AMR.337.358.

[15] H. Y. Dong, C. Y. Hu, G. H. Wu, K. M. Wu, and R. D. K. Misra, "An effect of nickel on hardening behavior and mechanical properties of nanostructured bainite-austenite steels," *Mater. Sci. Eng.*, vol. 817, pp. 141410, 2021. Doi: 10.1016/j.msea.2021.141410.

[16] Z. Yao, W. Dai, B. Cai, C. Li, H. Zhang, and Y. Zhang, "Effect of quenching temperature on tensile strength and fatigue behavior of an EA4T steel," *J. Mater. Eng. Perform.*, vol. 30, no. 12, pp. 9015-9028, 2021. Doi: 10.1007/s11665-021-06117-0.

[17] H. Jo, M. Kang, G. Park, B. Kim, C. Y. Choi, H. S. Park, S. Shin, W. Lee, Y. Ahn, and J. B. Jeon., "Effects of cooling rate during quenching and tempering conditions on microstructures and mechanical properties of carbon steel flange," *Materials (Basel)*, vol. 13, no. 18, pp. 1-16, 2020. Doi: 10.3390/MA13184186.

[18] B. Laxmi, S. Sharma, J. PK, and A. Hegde, "Quenchant oil viscosity and tempering temperature effect on mechanical properties of 42CrMo4 steel," *J. Mater. Res. Technol.*, vol. 16, pp. 581-587, 2022. Doi: 10.1016/j.jmrt.2021.11.152.

[19] P. Singh and S. Singh, "Effect of quenching media on microstructural evolution, mechanical and wear properties of AISI4135 steel," *Proc. Inst. Mech. Eng. Part C J. Mech. Eng. Sci.*, vol. 235, no. 21, pp. 5616-5625, 2021. Doi: 10.1177/0954406221990050.

[20] C. Baron, H. Werner, and H. Springer, "On the effect of carbon content and tempering on mechanical properties and stiffness of martensitic Fe–18.8Cr–1.8B–

xC high modulus steels," *Mater. Sci. Eng. A*, vol. 809, 2020, pp. 141000, 2021. Doi: 10.1016/j.msea.2021.141000.

[21] M. Grade and L. Carbon, "The effect of nickel contents on the microstructure evolution deposited metal," *Crystals*, vol. 11, no. 709, pp. 1-16, 2021.

[22] J. Wang, X. Di, C. Li, and D. Wang, "The influence of ni on bainite/martensite transformation and mechanical properties of deposited metals obtained from metal-cored wire," *Metals (Basel).*, vol. 11, no. 12, 2021. Doi: 10.3390/met11121971.

[23] C. G. Norwood, "The effect of nickel content on the mechanical properties and microstructure of a high toughness secondary hardening steel," Carnegie Mellon University, pp. 45, 2016.

[24] N. Alharthi, E. S. M. Sherif, H. S. Abdo, and S. Z. El Abedin, "Effect of nickel content on the corrosion resistance of iron-nickel alloys in concentrated hydrochloric acid pickling solutions," *Adv. Mater. Sci. Eng.*, vol. 2017, article no. 1893672, 2017. Doi: 10.1155/2017/1893672.

[25] Z. Li, W. Xue, Y. Chen, W. Yu, and K. Xiao, "Microstructure and grain boundary corrosion mechanism of pearlitic material," *J. Mater. Eng. Perform.*, vol. 31, no. 1, pp. 483-494, 2022. Doi: 10.1007/s11665-021-06171-8.

[26] D. Zhang, X. Gao, G. Su, Z. Liu, N. Yang, L. Du, and R. D. K. Misra, "Effect of tempered martensite and ferrite/bainite on corrosion behavior of low alloy steel used for flexible pipe exposed to high-temperature brine environment," *J. Mater. Eng. Perform.*, vol. 27, no. 9, pp. 4911-4920, 2018. Doi: 10.1007/s11665-018-3587-0.

[27] I. Bösing, I. Bobrov, J. Epp, M. Baune, and J. Thöming, "Influence of systematically changed martensite content on the passive film properties of austenitic stainless steel in neutral electrolyte," *Int. J. Electrochem. Sci.*, vol. 15, no. 1, pp. 319-333, 2020. Doi: 10.20964/2020.01.09.